AN OPTIMUM DESIGN STUDY OF INTERLACING NOZZLE BY ANALYZING FLUID FLOW INSIDE INTERLACING NOZZLES

Makhsuda Juraeva[1*], Kyung Jin Ryu[1], Sang Dug Kim[2], Dong Joo Song[2]

Air interlacing serves to protect the yarn against damage, strengthens inter-filament compactness or cohesion, and ensures fabric consistency. The air interlacing nozzle is used to introduce intermittent nips to a filament yarn so as to improve its performance in textile processing. This study investigates the effect of interlacing nozzle geometry on the interlacing process. The geometries of interlacing nozzles with multiple air inlets located across the width of a yarn channels are investigated. The basic interlacing nozzle is the yarn channel, with a perpendicular single air inlet in the middle. The yarn channel shapes are cross sections with semicircular or rectangular shapes. This paper presents three doubled sub air inlets with main air inlet and one of them is slightly inclined doubled sub air inlets with main air inlet. The compressed air coming out from the inlet hits the opposing wall of the yarn channel, divides into two branches, flows trough the top side of yarn channel, joins with the compressed air coming out from the sub air inlet and then creates two free jets at both ends of the yarn channel. The compressed air moves in the shape of two opposing directional vortices. The CFD-FASTRAN was used to perform steady simulations of impinging jet flow inside of the interlace nozzles. The vortical structure and the flow pattern such as pressure contour, particle traces, velocity vector plots inside of interlace nozzle geometry are discussed in this paper.

Key Words: An air inlet, yarn channel, CFD-FASTRAN, vorticity strength

1. Introduction

Interlacing is the process of yarn treatment, at the beginning of the process, filament yarns are flat and the filament bundle is completely open. The individual filaments of the yarn, while entering the air interlacer, are separated by the airflow and are set in rotation. Through this an accumulation of false-twist sections is created at the entrance as well as at the exit of the compressed air coming out from the air inlet, and these sections are called knots, or nodes. As the interlaced yarn is moving through the compressed air, the formed knot moves toward the air inlets and consequently, the rotation of the filaments is stopped. This process repeats itself periodically.

Interlacing influences the yarn structure and it is one of the advantage of interlacing. Schubert[1] found that a single air inlet leads to a higher nip frequency than multiple air inlets with the same air consumption. He found that an oblique air inlet increases nip frequency but disturbs yarn tension. Most researchers used simple air inlet configuration as a starting point to improve nip frequency.

There are different air interlacing techniques, tangling or intermingling, soft-interlacing and continuous interlacing. The operating principle of the continuous interlacing technology is based on two opposing air inlets, which are arranged at a defined angle to one another.

A new Y- interlacing technology is based on special flow air inlet geometry and its location in the air inlet. The two small side branches of the Y-cross sectional air flow transport the yarn into the middle of the channel to the front of the main air inlet in the interlacing zone[2].

In case of high performance interlacing jets and an average Polyester filament dpf (Denier per filament) of 3, up to 2,200 knots per second are formed. In case of micro-filaments this may be even 3,500 knots per second or more. Air interlacing provides assurance in the downstream performance of the yarn in weaving, knitting or warp knitting, without changing the other yarn properties.

1 Graduate student, School of Mechanical Engineering, Yeungnam University
2 Professor, School of Mechanical Engineering, Yeungnam University
* Corresponding author E-mail: mjuraeva@yumail.ac.kr

2. Computation Methods

Computational Fluid Dynamics (CFD) have become a vital part of design and analysis in both research and commercial industries. CFD offers the ability to make a very detailed and thorough study of flow-fields and is capable of solving a broad range of flow problems. The Navier-Stokes equations are solved with the choice of turbulence model. Though turbulent flows are governed by Navier-Stokes equations, the wide range of length and time scales poses difficulties in treating turbulence both analytically and numerically. The choice of turbulence model will depend on considerations such as the physics encompassed in the flow, the established practice in a specific class of problem, the level of accuracy required, the available computational resources, and the amount of computing time available.

2.1 Spalart-Allmaras Model, Inviscid (Euler) and Laminar flow

The Spalart-Allmaras model is a relatively simple one-equation model (Spalart and Allmaras 1992)[3]that solves a modeled transport equation for the kinematic eddy (turbulent) viscosity. This embodies a relatively new class of one-equation models in which it is not necessary to calculate a length scale related to the local shear layer thickness. This Model is a low Reynolds number model, which can be directly applied through out the boundary layer if the near wall mesh is fine enough to resolve the gradients.

The Euler equations are a subset of the Navier-Stokes equations with transport phenomena such as viscosity and heat condition terms set to zero.

Laminar flow requires additional parameters within the flow solver to determine viscous and conductive effects.

2.2 Computational Approach

The CFD-GEOM provides the geometry and modifies the geometry read through IGES or Plot3D data formats [4]. CFD-GEOM is used for initial problem set-up, definition of the prescribed motion of the geometry and structured grid topology of the problem, the geometry manipulation, and grid. CFD-FASTRAN is a parallel, implicit, Euler/Navier-Stokes Flow solver. This code is used to solve the high speed, highly separated flow problems. CFD-FASTRAN capabilities represent the culmination of the growing experiences of developing advanced simulation software and associated physical models[5]. CFD-VIEW is the 3D graphical post-processor that analyze CFD results[6]. One of the challenges in computational modeling is that each simulation generates a large volume of data which must be reduced to extract useful information to practical science and engineering problems. CFD-VIEW uses surface-based visualization. It can display one or more computational planes, cutting planes, walls, vector quantities by mapping small vector arrows on surface, particle tracing, surface contours, flooded contours and point probe.

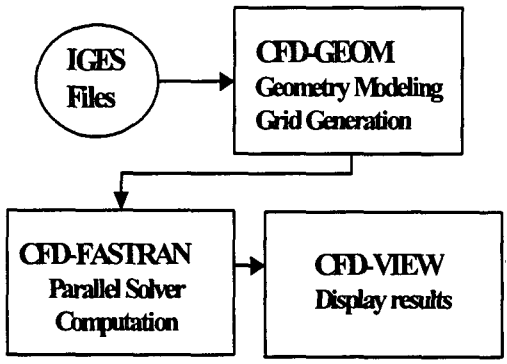

Figure 1. Overview of Computational approach

Figure 1 shows the various computational tools used in this approach. The results shown below for each case are created using CFD-VIEW.

2.3 Geometric Modeling and Grid Generation

This study investigates three test cases with multiple air inlets. There are doubled sub air inlets and oblique sub air inlets for the case 3. The yarn channel cross sections are semicircular and trapezoidal.

The geometry model and computational grid for the interlace nozzle were created using the CFD-GEOM software. The geometry model was based on an IGES CAD description. The modeled geometry consisted of yarn channel which connected with air inlets. The computational interlace nozzle geometry is cut twice vertically using symmetry. The symmetry allows the computational problem to be reduced by only modeling half of the geometry.

The mesh is adapted to the interlacing nozzle shape through an iterative procedure. The grid near the wall was clustered to capture the boundary layer and be consistent with the requirements of the turbulence model being used. Better grid distribution in these regions provide more accurate prediction of

the effects from flow features such as boundary layers, flow separation and vortices.

2.4 Boundary, Initial and Solver conditions for all cases

The boundary conditions are imposed as follows: "wall" on the yarn channel and air inlets body, "inlet" at the air inlets, "symmetry" on the symmetry plane, "outlet" at the end of yarn channel. All walls were treated as viscous adiabatic surfaces with a no-slip velocity condition. The outlet boundary was modeled using an extrapolated boundary condition to be applied at the exit that required no assumption about the local flow state.

The inlet condition for all cases is given as 2 and 3 atm pressure with zero inlet velocity, 288 K temperature and 0.0001529737 (m^2/s) turbulent viscosity for turbulent computation. Turbulent viscosity is not used for inviscid Euler and laminar flow computations. The remaining external boundaries were modeled with a symmetry condition.

The initial conditions for all cases volume are given 1 atm pressure with zero velocity, 288 K temperature and (0.0001529737 m^2/s) turbulent viscosity for turbulent computation.

Each case to be simulated is the turbulent flow. The fluid conductivity is based on a Prandtl number of 0.7. The turbulent conductivity is based on turbulent Prandtl number of 0.9. Sutherland's law viscosity option is used for computation.

The Roe's approximate Riemann Solver is referred to as a Flux Difference Scheme in the solver control. The Osher-Chakravarthy flux limiter provides up to third order spatial accuracy. High order spatial accuracy with the fully implicit scheme is used for computation. The initial CFL number (0.1) and final CFL number (1) are prescribed on the time integration scheme.

3. Results and Discussion

The computational analysis results of three cases are presented. The width and depth of yarn channel and the width of the sub air inlets are chosen case by case. Vortices of the compressed air are investigated. The compressed air coming out from the inlet hits the opposing wall of the yarn channel, divides into two branches, flows through the top side of yarn channel, joins with the compressed air coming out from the sub air inlet and creates vortices in the yarn channel.

3.1 Case 1

When main and sub air inlets have the same atmospheric pressure, the compressed air jet coming out from sub air inlet collides with the compressed air jet coming out from main air inlet, and suppresses flow motion. The main air inlet size is smaller than sub air inlet size. The compressed air jet coming out from the main air inlet gets influence in the lower part of yarn channel, moves to the center of yarn channel and makes sliding vortex motion.

We can see similar pressure distribution in all air inlets pressure. In this case, the low pressure domain moves to the center of yarn channel while pressure becomes higher. The pressure decreases while the compressed air flows to yarn channel exit direction. The pressure distributions are similar while total pressure is high.

3.2 Case 2

Figures 2 and 3 show computational flow analyses of cases 1, 2 and 3. All results are obtained with 2, 3 and 4 atm pressure in the air inlets. The compressed air from main air inlet hits the opposing wall of the yarn channel, divides into two branches and on the way meets the compressed air from sub air inlet which located at the top of yarn channel combined flow goes down through yarn channel wall and forms vortex. The air velocity vector is shown at the symmetry part of Case 2 in the Fig. 2. When we compare flow motions, the compressed air from the sub air inlet hits opposing side wall of yarn channel, flows along wall, makes stronger flow motion than Case 1. According to Case 1 results, the sub nozzle is near to the yarn channel side wall and the size is smaller. Some design parameters and computational results of Case 1 help to obtain optimum interlacing nozzle design.

We can see similar pressure distribution in all air inlet pressure. In this case, the center of low pressure domain is near to the side wall of yarn channel. High pressure forces relatively low pressure flow to rotate. The pressure decreases while the compressed air flows to yarn channel exit direction. The pressure distributions are similar while total pressure is high.

3.3 Case 3

The effect of air pressure is investigated with 2, 3 and 4 atm pressure in the air inlet. In this case sub air inlet is an inclined air inlet. The air jet from inclined air inlet hits the opposing side wall of the yarn channel, flows through the side wall and

results in high turbulence strength.

The pressure distributions are similar in all the air inlets. The center of low pressure domain is near the center of yarn channel. The sub air inlet flow reduces main air inlet flow while inlet pressure becomes higher. Computational results show smooth vortex motion for this case. Right side of sub air inlet has useless space which is inefficient in order to vortex strength. The pressure decreases while the compressed air flows to yarn channel exit direction. The pressure distributions are similar while total pressure is high. The streamlines of Cases 1, 2 and 3 has relatively high rotational motion than basic case while the compressed air flows to the yarn channel exit. The rotational flow motion of through the yarn channel and the central side of case 2 and 3 is relatively strong. The compressed air flow at the central side of Case 1 can have a forced motion because of bigger sub air inlet. Following table 1 presents vortex strength of Cases 2, 3, and 4 through (z - direction) yarn channel body. The A, B and C cuts are in the center, around connection part of air inlet and yarn channel. The Vorticity strength of case 3 is higher than case 4. If we compare mass flow rate of case 2 and 3 mass flow rate of case 3 is relatively smaller than case 2.

4. Conclusions

The compressed air coming out from main air inlet and sub air inlets form vortex flow motion inside of the yarn channel. In Case 1, the compressed air coming out from sub air inlet reduces the compressed air from main air inlet and makes vortex. The sub air inlets are quite big and not near to the side wall of yarn channel.

In Case 2 the sub air inlets are moved to the side wall of the yarn channel, and the size is smaller than before. We can observe the compressed air from sub air inlet moves flow motion to the center of the yarn channel and flows strongly through the side wall of the yarn channel. If we compare the Vorticity strength of Cases 2 and 3, the Vorticity strength of case 3 is relatively smaller than Case 2.

Case 3 has the inclined air inlet which drives flow to go through the side wall of yarn channel. The compressed air from the sub air inlet hits the opposing the side wall of the yarn channel and makes vortical motion. The right side of the sub air inlet has dead zone. We will continue our optimum design study based on computational results of Cases 2 and 3.

References

[1] Schubert, G., 1980, Vortexting of Flat Yarns, Chemiefas, Textilind. 30/82(10), 820-823. E92-93.

[2] M. A. Zenses, Y and CI Air Jets - Air Interlacing Technology for Different Textile Processes, Chemical Fiber International, Volume 53, February 2003.

[3] Spalart, P.R. and Allmaras, S.R. "A One-equation Turbulence Model for Aerodynamic Flows". AIAA Paper 92-0439, American Inst. of Aeronautics and Astronautics, 1992.

[4] CFD-GEOM Version 2004 User's Manual, CFD Research Corporation, Huntsville, AL.

[5] CFD-FASTRAN Version 2002, User's Manual, CFD Research Corporation, Huntsville, AL.

[6] CFD-VIEW Version 2002, User's Manual, CFD Research Corporation, Huntsville, AL.

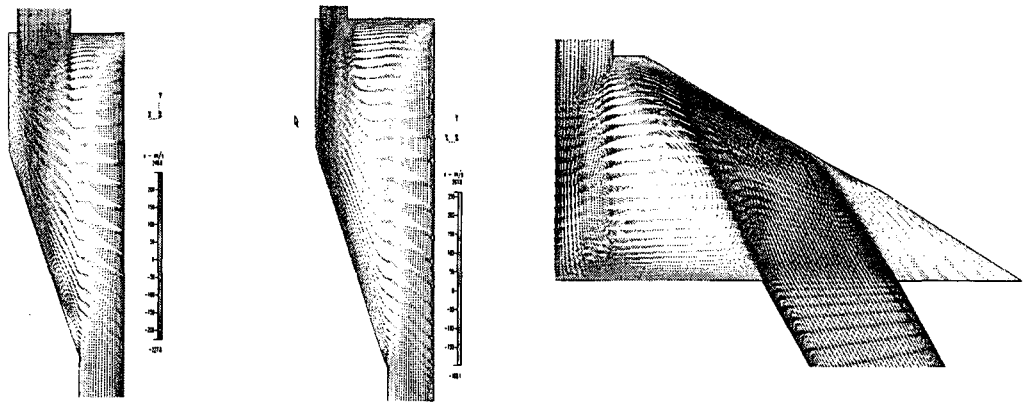

Figure 2. Velocity vector plot for case 1, 2 and 3 (at 2 atm pressure)

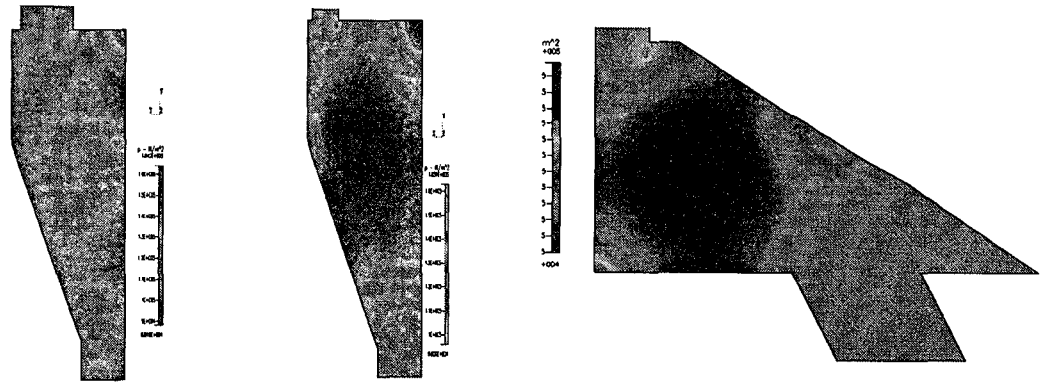

Figure 3. Pressure contour plot of case 1, 2 and 3 (at 2 atm pressure)

Table 1 Vorticity strength of case1,2 and 3.

Vorticity strength	case 1			case 2			case 3		
Inlet pressure	2 atm	3 atm	4 atm	2 atm	3 atm	4 atm	2 atm	3 atm	4 atm
A cut	7556	9758	10850	9935	12631	13878	3746	4790	5383
B cut	9381	12280	13869	8625	11063	12981	3012	4113	4810
C cut	4101	5969	7406	1865	2518	3070	2140	2943	3446